

Visual Cortical Neurons Depolarize after Hippocampal Ripples

Hana Samejima¹, Yu Sato¹, Yuji Ikegaya^{1,2,3*}

¹Graduate School of Pharmaceutical Sciences, The University of Tokyo, Tokyo 113-0033, Japan

²Institute for AI and Beyond, The University of Tokyo, Tokyo 113-0033, Japan

³Center for Information and Neural Networks, National Institute of Information and Communications Technology, Suita City, Osaka, 565-0871, Japan

*Corresponding Author

Yuji Ikegaya, Laboratory of Chemical Pharmacology, Graduate School of Pharmaceutical Sciences, The University of Tokyo, 7-3-1 Hongo, Bunkyo-ku, Tokyo 113-0033, Japan.

Submitted: 30 Dec 2022; **Accepted:** 05 Jan 2023; **Published:** 12 Jan 2023

Citation: Samejima, H., Sato, Y., & Ikegaya, Y. (2023). Visual Cortical Neurons Depolarize after Hippocampal Ripples. *New Adv Brain & Critical Care*, 4(1), 01-05.

Abstract

Objective: When memory is consolidated, the hippocampus emits brief high-frequency oscillations called ripples, which often occur simultaneously with slow waves in the neocortex. Long-term visual memory consolidation requires neuronal coordination between the hippocampus and the primary visual cortex (V1). However, little is known about the dynamics of the membrane potentials of neocortical neurons during hippocampal ripples. The aim of this study is to reveal the subthreshold activity in individual V1 neurons during hippocampal ripples.

Methods: We patch-clamped V1 layer 2/3 pyramidal cells and monitored their membrane potentials while also recording local field potentials from the hippocampal CA1 region in anesthetized mice.

Results: Approximately 20% of V1 neurons were transiently depolarized 18–45 ms after the onset of ripples that occurred in neocortical UP states. The depolarization magnitudes were not correlated with the durations, frequencies, or powers of ripples.

Conclusions: Hippocampal ripples are associated with the subthreshold dynamics of V1 neurons, despite the lack of direct synaptic connections between the hippocampus and the V1.

Keywords: Visual Cortex, Hippocampal Ripple, Membrane Potential, Slow Wave, Whole-Cell Recording

Introduction

Neuronal coordination between the hippocampus and the neocortex plays an essential role in consolidating memory traces in the neocortex [1]. During behaviorally inactive states, non-rapid eye movement (NREM) sleep, and anesthesia, spontaneous activity in the neocortex is dominated by slow waves, which are low-frequency (0.5–4 Hz) oscillations in local field potentials (LFPs) that alternate slowly between active periods (UP states) and silent periods (DOWN states) [2,3]. During slow-wave activity, the hippocampus emits sharp-wave ripples, a form of high-frequency (150–250 Hz) oscillation [4,5]. Active communications between the hippocampus and the neocortex during NREM sleep are believed to be instrumental in memory consolidation [6,7].

The primary visual cortex (V1) is the first neocortical region to receive visually relevant input and is involved in long-term visual

recognition memory [8,9]. Although there are no direct synaptic interactions between the hippocampus and the V1, these two brain regions exhibit functional connectivity [10,11]. For example, V1 neurons undergo coherent reactivation in conjunction with memory replays during hippocampal ripples [12]. Wide-field optical imaging and extracellular unit recordings have demonstrated that V1 neurons fire spikes around hippocampal ripples [13,14]. However, it remains unclear what percentage of V1 neurons respond to ripples and how the subthreshold dynamics of their membrane potentials V_m s are modulated by ripples.

In the present study, we hypothesized that spontaneously occurring ripples exert a functional impact on V1 neuronal activity and that this interaction is reflected in the subthreshold V_m dynamics of V1 neurons. Using in vivo whole-cell recording techniques and extracellular field recording techniques, we recorded V_m s from

layer 2/3 pyramidal cells in the V1 simultaneously with LFPs from the CA1 *stratum pyramidale* in the hippocampus. We found that V1 neurons were depolarized after ripples that occurred during UP states and that the duration, frequency, and power of ripples were not correlated with the V1 depolarization sizes.

Materials and Methods

Animals

The animal experiments were performed with the approval of the Animal Experiment Ethics Committee at The University of Tokyo (approval number: P4-2) and according to the University of Tokyo guidelines for the care and use of laboratory animals. These experimental protocols were carried out in accordance with the Fundamental Guidelines for Proper Conduct of Animal Experiment and Related Activities in Academic Research Institutions (Ministry of Education, Culture, Sports, Science and Technology, Notice No. 71 of 2006), the Standards for Breeding and Housing of and Pain Alleviation for Experimental Animals (Ministry of the Environment, Notice No. 88 of 2006) and the Guidelines on the Method of Animal Disposal (Prime Minister's Office, Notice No. 40 of 1995). Postnatal 28- to 40-day-old male ICR mice (Japan SLC, Shizuoka, Japan) were housed on a 12/12-h light-dark cycle (light from 06:00 to 18:00) at 22 ± 1 °C with food and water provided ad libitum and were used in the experiments.

Electrophysiology

After exposure to a cage enriched with toys for 30 min, mice were intraperitoneally anesthetized with 2.25 g/kg urethane. Anesthesia was confirmed by the absence of paw withdrawal, whisker movement, and eyeblink reflexes. The skin was subsequently removed from the head, and a metal head-holding plate was fixed to the skull. A craniotomy of 2.0×2.0 mm² was performed; it was centered at 3.0 mm posterior to the bregma and 2.5 mm ventrolateral to the sagittal suture. The exposed neocortical window was covered with 2.0% agar at a thickness of 2.0 mm. LFPs were recorded from the dorsal hippocampal CA1 region using a tungsten electrode (3.5–4.5 M Ω , catalog #UEWMGCSEKNNM, FHC, USA) coated with a crystalline powder of 1,1'-dioctadecyl-3,3',3'-tetramethylindocarbocyanine perchlorate (DiI). Whole-cell recordings were obtained from layer 2/3 neurons in the V1 (AP: 2.0–5.0 mm posterior to bregma; ML: 1.2–3.0 mm from the sagittal suture; DV: 0–0.8 mm ventral to the dura) using borosilicate glass electrodes (3–8 M Ω). Pyramidal cells were identified based on regular spiking properties in response to step-pulse current injection and *post hoc* histological analysis. Cells were discarded unless they were identified as pyramidal cells. The intrapipette solution consisted of the following reagents: 120 mM K-gluconate, 10 mM KCl, 10 mM HEPES, 10 mM creatine phosphate, 4 mM MgATP, 0.3 mM Na₂GTP, 0.2 mM EGTA (pH 7.3), and 0.2% biocytin. Liquid junctions were corrected offline. Cells were discarded when the mean liquid resting V_m exceeded -55 mV or when the action potentials were below -20 mV. Signals recorded with tungsten electrodes and glass electrodes were amplified using a DAM80 AC differential amplifier and a MultiClamp 700B amplifier, re-

spectively. Both types of signals were digitized at a sampling rate of 20 kHz using a Digidata 1440A digitizer that was controlled by pCLAMP 10.3 software (Molecular Devices).

Histology

Following each experiment, the electrodes were carefully withdrawn. The mice were transcardially perfused with 4% paraformaldehyde, and the brains were postfixed overnight with paraformaldehyde. The brains were coronally sectioned at a thickness of 100 μ m using a vibratome. The sections were incubated with 2 μ g/ml streptavidin-Alexa Fluor 594 conjugate and 0.2% Triton X-100 for 4 h, followed by incubation with 0.4% NeuroTrace 435/455 Blue Fluorescent Nissl Stain (Thermo Fisher Scientific; N21479) for 1.5–4 h. Fluorescent images were acquired using a confocal microscope (A1 HD25, Nikon, Tokyo, Japan) and were subsequently merged.

Data Analysis

Data were analyzed offline using custom-made MATLAB (R2021a, Natick, Massachusetts, USA) routines. For correlation plots, the significance was determined based on Pearson's correlation coefficient and *t*-test of the correlation coefficients. $P < 0.05$ was considered statistically significant. All statistical tests were two-sided. To detect ripples from LFP traces recorded with a tungsten electrode, LFP traces were downsampled to 2 kHz and bandpass filtered between 150 and 250 Hz. Ripples and their onset and offset time points were detected at a threshold of $4 \times$ SD of the baseline noise. The detected events were subsequently scrutinized by eye and manually rejected if the detection was erroneous. We analyzed only datasets that included at least 50 ripple events. The oscillatory frequency of ripples was computed using complex Morlet wavelets of LFPs. The ripple power was calculated as the square of the difference of maximum and minimum LFP between the onset and offset of the ripple.

For each ripple, we averaged V_m between -100 ms and 100 ms from the ripple onset time; this average was designated \bar{V}_m . For a given time point within this window, we considered the difference between V_m and \bar{V}_m as $V_m - \bar{V}_m$. We obtained the $V_m - \bar{V}_m$ traces for all ripples and averaged them by alignment to the ripple onsets as the onset-triggered average. To estimate the chance levels of the triggered average, we also computed $V_m - \bar{V}_m$ traces for 10,000 randomly selected 200-ms periods and defined the top 2.5% to 97.5% as the 95% confidence interval. If any time point between 0 and 100 ms from the ripple onset in a given ripple exceeded the 95% confidence interval, the V_m response was considered depolarization. We then identified the time point that gave the maximum $V_m - \bar{V}_m$ between 0 and 100 ms from the ripple onset time and defined $V_m - \bar{V}_m$ at this time point as ΔV_m .

Results

We obtained whole-cell current-clamp recordings from a total of 29 layer 2/3 pyramidal cells in the V1 from 25 urethane-anesthetized mice while monitoring LFPs from the hippocampal CA1 region (Figure 1A). The mean recording period was 972 ± 607 sec (mean \pm SD), during which 114 ± 85 ripple events were detected (Figure 1B).

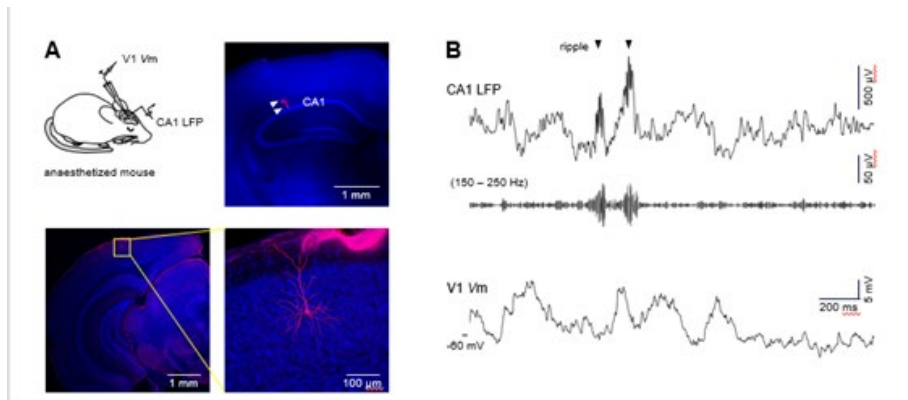


Figure 1: Simultaneous recordings of hippocampal LFPs and V_m of V1 layer 2/3 pyramidal cells

(A) Top left: Schematic depiction of an LFP recording from the hippocampal CA1 region and a whole-cell recording from a V1 neuron. Top right: A track of a DiI-coated electrode for LFP recording in a Nissl stained coronal section. Scale bars, 1 mm. Bottoms: A post hoc biocytin-based identification of a recorded neuron in a Nissl stained coronal section. The boxed area in the left panel is magnified in the right panel. Bottom Left: Scale bars, 1 mm. Bottom Right: $\sim 100\mu\text{m}$

(B) Representative traces of hippocampal LFPs, 150–250 Hz bandpass-filtered LFPs, and V_m of a V1 pyramidal cell

Subthreshold V_m s from single V1 neurons were averaged relative to each ripple onset and compared to their change levels estimated from 10,000 resampled surrogate data (Figure 2A second row). Of the 29 V1 neurons recorded, 2 (7%) exhibited significant depolarization after the ripple onsets (Figure 2B top). Because neocortical neurons fluctuate between depolarized (UP) and hyperpolarized

(DOWN) states under urethane anesthesia, V_m s were averaged separately for cortical UP and DOWN states (Fig. 2A third row and bottom) [9]. When ripples occurred during V1 UP states, 6 of 29 (21%) neurons were significantly depolarized after the ripple onsets (Figure 2B middle), whereas 1 of 29 (3%) cells was depolarized during DOWN states (Figure 2B bottom).

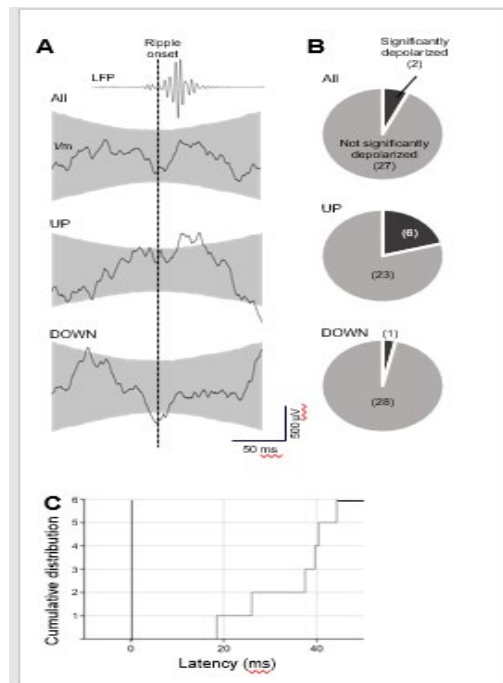


Figure 2: V1 neurons depolarize after hippocampal ripples during UP states

(A) Top: The average waveform of ripples recorded from a mouse. Second row: ΔV_m relative to the ripple onset timings was averaged for all ripples recorded in a single neuron. Gray areas indicate the 95% confidence intervals. Third row and bottom: the same as the second row but for ripples during UP states and DOWN states, respectively, in the same neuron.

(B) The distributions of V1 neurons that significantly depolarized in response to ripples versus those that did not respond to ripples. $n = 29$ cells.

(C) Latencies of V1 depolarizations during UP states relative to the ripple onsets. $n = 6$ cells.

The latencies of the depolarizations that occurred during UP states in 6 V1 neurons from the ripple onsets was 34.4 ± 9.9 ms (mean \pm SD), ranging from 18.5 to 44.3 ms, suggesting polysynaptic transmission from the hippocampus to the V1 (Figure 2C, $n = 6$ cells from 6 mice).

Finally, we investigated whether the depolarization sizes (ΔV_m) were correlated with the properties of individual ripples, such as their duration, oscillatory frequency, or power (Fig. 3A). None of these parameters had significant correlations with ΔV_m (Fig. 3B; duration: $R = 0.001$, $P = 0.987$; frequency: $R = -0.020$, $P = 0.705$; power: $R = 0.034$, $P = 0.521$ t -test, $n = 362$ from 6 cells).

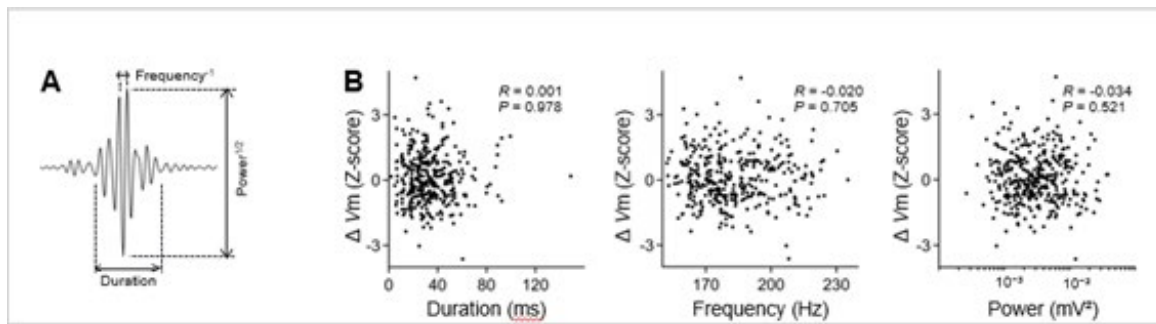


Figure 3: Lack of correlations between V1 ΔV_m and hippocampal ripples

(A) Schematic depictions for the definitions of the duration, frequency, and power of a ripple.

(B) Relationships between ΔV_m and the duration (left), frequency (middle), and power (right) of ripples that occurred during UP states. Each dot indicates a single ripple event. Statistical comparisons were conducted using t -tests of the correlation coefficients. $n=362$ ripples from 6 cells

Discussion

A previous work using wide-field optical imaging in mice indicated that the visual cortex, including the V1, showed spatiotemporally complicated peri-ripple activation [13]. Our result showing that ripples preceded V1 depolarization confirms this observation and supports that there is an information pathway from the hippocampus to the V1. The latencies of V1 depolarizations were approximately 18–45 ms and long enough to be assumed to reflect multiple synaptic steps, consistent with the fact that the hippocampus has no direct synaptic connection with the V1. The shortest known route anatomically connecting these two brain regions is a trisynaptic pathway consisting of the hippocampus, the subiculum, the retrosplenial cortex, and the V1 [11,15].

Neocortical UP states are characterized by depolarized V_m and vibrant synaptic barrages, whereas DOWN states are characterized by hyperpolarized V_m and scarce synaptic activity [16]. V_m s are suggested to reflect the influence of synaptic inputs more during UP states than during DOWN states [17]. Assuming that ripples gate information transmission from the hippocampus to the V1, this idea is consistent with our findings that V1 depolarizations were more prominent during UP states. A previous study reported that neocortical spiking activity after ripples is inversely related to the magnitude of ripples [14]. On the other hand, we found that ΔV_m s in V1 neurons was not correlated with the features of ripples; that is, there was no simple relationship such that larger ripples caused larger depolarizations. These results suggest that complex neural processing occurs in the transmission of information from the hippocampus to the V1.

Hippocampal ripples are important for memory consolidation, in which the hippocampus is believed to guide reorganization of information stored in the neocortex through offline replays of sequential firings of memory-encoding neurons during ripples [18]. The V1 also shows coherent reactivation with hippocampal replays during ripples [19]. Our findings advance the current understanding of neuronal mechanisms underlying the consolidation of visual memories.

Conclusion

In conclusion, we investigated V1 neuronal V_m activity during hippocampal ripples and found that a portion of V1 neurons were depolarized after hippocampal ripples that occurred during UP states; furthermore, we found that the ripple duration, frequency, and power were not correlated with the amplitudes of post-ripple depolarizations of V1 neurons. Our findings not only expand previous knowledge about mutual interaction between hippocampal and extrahippocampal brain circuits, especially its connection to the V1, but also illustrate neocortical subthreshold V_m dynamics triggered by hippocampal ripples.

Acknowledgments

This work was supported by JST ERATO (JPMJER1801), Institute for AI and Beyond of the University of Tokyo, and JSPS Grants-in-Aid for Scientific Research (18H05525).

References

1. Sekeres, M. J., Winocur, G., & Moscovitch, M. (2018). The hippocampus and related neocortical structures in memory transformation. *Neuroscience letters*, 680, 39-53.

2. Miyamoto, D., Hirai, D., & Murayama, M. (2017). The roles of cortical slow waves in synaptic plasticity and memory consolidation. *Frontiers in neural circuits*, 11, 92.
3. Cowan, R. L., & Wilson, C. J. (1994). Spontaneous firing patterns and axonal projections of single corticostriatal neurons in the rat medial agranular cortex. *Journal of neurophysiology*, 71(1), 17-32.
4. Girardeau, G., Benchenane, K., Wiener, S. I., Buzsáki, G., & Zugaro, M. B. (2009). Selective suppression of hippocampal ripples impairs spatial memory. *Nature neuroscience*, 12(10), 1222-1223.
5. Norimoto, H., Makino, K., Gao, M., Shikano, Y., Okamoto, K., Ishikawa, T., ... & Ikegaya, Y. (2018). Hippocampal ripples down-regulate synapses. *Science*, 359(6383), 1524-1527.
6. Mainjret, N., Girardeau, G., Todorova, R., Goutierre, M., & Zugaro, M. (2016). Hippocampo-cortical coupling mediates memory consolidation during sleep. *Nature neuroscience*, 19(7), 959-964.
7. Todorova, R., & Zugaro, M. (2019). Isolated cortical computations during delta waves support memory consolidation. *Science*, 366(6463), 377-381.
8. Siegle, J. H., Jia, X., Durand, S., Gale, S., Bennett, C., Gradis, N., ... & Koch, C. (2021). Survey of spiking in the mouse visual system reveals functional hierarchy. *Nature*, 592(7852), 86-92.
9. Cooke, S. F., & Bear, M. F. (2015). Visual recognition memory: a view from V1. *Current opinion in neurobiology*, 35, 57-65.
10. Hindy, N. C., Avery, E. W., & Turk-Browne, N. B. (2019). Hippocampal-neocortical interactions sharpen over time for predictive actions. *Nature communications*, 10(1), 1-13.
11. Makino, H., & Komiyama, T. (2015). Learning enhances the relative impact of top-down processing in the visual cortex. *Nature neuroscience*, 18(8), 1116-1122.
12. Foster, D. J., & Wilson, M. A. (2007). Hippocampal theta sequences. *Hippocampus*, 17(11), 1093-1099.
13. Abadchi, J. K., Nazari-Ahangarkolaee, M., Gattas, S., Bermudez-Contreras, E., Luczak, A., McNaughton, B. L., & Mohajeri, M. H. (2020). Spatiotemporal patterns of neocortical activity around hippocampal sharp-wave ripples. *Elife*, 9, e51972.
14. Nitzan, N., Swanson, R., Schmitz, D., & Buzsáki, G. (2022). Brain-wide interactions during hippocampal sharp wave ripples. *Proceedings of the National Academy of Sciences*, 119(20), e2200931119.
15. Ferreira-Fernandes, E., Pinto-Correia, B., Quintino, C., & Remondes, M. (2019). A gradient of hippocampal inputs to the medial mesocortex. *Cell reports*, 29(10), 3266-3279.
16. Mölle, M., & Born, J. (2011). Slow oscillations orchestrating fast oscillations and memory consolidation. *Progress in brain research*, 193, 93-110.
17. Waters, J., & Helmchen, F. (2006). Background synaptic activity is sparse in neocortex. *Journal of Neuroscience*, 26(32), 8267-8277.
18. Buzsáki, G. (2015). Hippocampal sharp wave-ripple: A cognitive biomarker for episodic memory and planning. *Hippocampus*, 25(10), 1073-1188.
19. Ji, D., & Wilson, M. A. (2007). Coordinated memory replay in the visual cortex and hippocampus during sleep. *Nature neuroscience*, 10(1), 100-107.

Copyright: ©2023 Yuji Ikegaya, et. al. This is an open-access article distributed under the terms of the Creative Commons Attribution License, which permits unrestricted use, distribution, and reproduction in any medium, provided the original author and source are credited.